Inorg. Chem. **2006**, *45*, 8648–8654

Infrared Spectra of the $M(NO)_n$ (M = Sn, Pb; n = 1, 2) and $PbNO^-$ Molecules

Qiang Xu* and Ling Jiang

National Institute of Advanced Industrial Science and Technology (AIST), Ikeda, Osaka 563-8577, Japan, and Graduate School of Science and Technology, Kobe University, Nada Ku, Kobe, Hyogo 657-8501, Japan

Received June 20, 2006

Reactions of laser-ablated tin and lead atoms with nitric oxide molecules in solid argon and neon have been investigated using matrix-isolation infrared spectroscopy. In the argon experiments, absorptions at 1560.1, 1625.8, and 1486.7 cm^{-1} are assigned to the N–O stretching vibrations of the SnNO and $Sn(NO)_2$ molecules, and absorptions at 1541.9, 1630.0, 1481.8, and 1457.5 cm^{-1} are assigned to the N–O stretching vibrations of the PbNO, $Pb(NO)_2$, and $PbNO^-$ molecules on the basis of isotopic shifts and splitting patterns. The present neon experiments only produce neutral tin and lead mononitrosyls. Density functional theory calculations have been performed on these tin and lead nitrosyls. The good agreement between the experimental and calculated vibrational frequencies, relative absorption intensities, and isotopic shifts substantiates the identification of these nitrosyls from the matrix infrared spectra.

Introduction

The interaction of nitric oxide with metal atoms is of considerable interest from an academic or an industrial viewpoint because nitric oxides are the main pollutants in the fuel combustion process, and their removal involves catalytic reduction on the metal surface.[1] On the other hand, nitric oxide has been found to play as a signaling molecule in biological systems.[1] Extensive experimental and theoretical investigations have been explored to understand the adsorption and reduction of nitric oxide on group 14 metal surfaces. It seems established that NO adsorbs both molecularly and dissociatively on Si(111)7×7 at 90 K and the photogenerated charge carriers in Si initiate the photodesorption and photodissociation of molecularly adsorbed NO.[2] Similarly, the germanium surface has been found to be also quite reactive toward NO.[3] Previous investigations show that the Rh−Sn/SiO_2 catalysts prepared by the reaction of $Sn(CH_3)_4$ with Rh/SiO_2 have a much higher activity for NO dissociation and catalytic NO−H_2 reaction than a monometallic Rh/SiO_2 catalyst and a coimpregnation Rh−Sn/SiO_2 catalyst.[4] Also, it has been found that modification of 6 wt % Co/Al_2O_3 with 2 wt % Sn significantly enhanced the catalyst thermal stability and improved the inhibitory effect of water on NO conversion and reaction temperature.[5] Alloying Sn into the surface layer of Pt(100) reduces the adsorption energy of molecularly bound NO by more than a factor of 2 and completely changes the NO reaction pathway.[6]

Recent studies have shown that, with the aid of isotopic substitution, matrix isolation infrared spectroscopy combined with quantum chemical calculation is very powerful in investigating the spectrum, structure, and bonding of novel species.[7−9] Argon matrix investigations of the reaction of laser-ablated Si atoms and NO molecules have characterized

* Author to whom correspondence should be addressed. Phone: 81 727-51-9652. Fax: 81 727-51-9629. E-mail: q.xu@aist.go.jp.

(1) Richter-Addo, G. B.; Legzdins, P.; Burstyn, J. *Chem. Rev*. **2002**, *102* (4, thematic issue on nitric oxide chemistry).
(2) Ying, Z.; Ho, W. *Phys. Rev. Lett*. **1988**, *60*, 57.
(3) See, for example: Modl, A.; Gritsch, T.; Budde, F.; Chuang, T. J.; Ertl, G. *Phys. Rev. Lett*. **1986**, *57*, 384. Ranke, W.; Chen, X. H.; Schroder-Bergen, E. *Vacuum* **1990**, *41*, 656.
(4) Tomishige, K.; Asakura, K.; Iwasawa, Y. *J. Chem. Soc., Chem. Commun*. **1993**, 184.
(5) Chen, L. Y.; Horiuchi, T.; Mori, T. *Catal. Lett*. **2001**, *72*, 71.
(6) Panja, C.; Koel, B. E. *J. Phys. Chem. A* **2000**, *104*, 2486.
(7) See, for example: Xu, C.; Manceron, L.; Perchard, J. P. *J. Chem. Soc., Faraday Trans*. **1993**, *89*, 1291. Bondybey, V. E.; Smith, A. M.; Agreiter, J. *Chem. Rev*. **1996**, *96*, 2113. Fedrigo, S.; Haslett, T. L.; Moskovits, M. *J. Am. Chem. Soc*. **1996**, *118*, 5083. Khriachtchev, L.; Pettersson, M.; Runeberg, N.; Lundell, J.; Rasanen, M. *Nature* **2000**, *406*, 874. Himmel, H. J.; Manceron, L.; Downs, A. J.; Pullumbi, P. *J. Am. Chem. Soc*. **2002**, *124*, 4448. Li, J.; Bursten, B. E.; Liang, B.; Andrews, L. *Science* **2002**, *295*, 2242. Andrews, L.; Wang, X. *Science* **2003**, *299*, 2049.
(8) Andrews, L.; Citra, A. *Chem. Rev*. **2002**, *102*, 885. Himmel, H. J.; Downs, A. J.; Greene, T. M. *Chem. Rev*. **2002**, *102*, 4191 and references therein.

10.1021/ic061105r CCC: $33.50
Published on Web 09/16/2006

three different isomers of SiNO (i.e., the end-bonded nitrosyl SiNO, the side-bonded nitrosyl *cyc*-SiNO, and the inserted product NSiO) and the $Si(NO)_2$ and SiNSiO molecules.[10] Similarly, the $Ge(NO)_n$ ($n = 1, 2$) and $GeNO^-$ molecules have been identified from isotopic shifts and splitting patterns in the argon matrix infrared spectra.[11] However, almost nothing is known about simple tin or lead nitrosyl molecules. Here, we report a study of the reactions of laser-ablated tin and lead atoms with NO molecules in excess argon and neon. IR spectroscopy coupled with theoretical calculations provides evidence for the formation of the $M(NO)_n$ (M = Sn, Pb; $n = 1, 2$) and $PbNO^-$ molecules.

Experimental and Theoretical Methods

The experiment for laser ablation and matrix isolation infrared spectroscopy is similar to those previously reported.[12,13] Briefly, the Nd:YAG laser fundamental (1064 nm, 10 Hz repetition rate with 10 ns pulse width) was focused on the rotating Sn and Pb targets. The laser-ablated Sn and Pb atoms were co-deposited with NO in excess argon (or neon) onto a CsI window cooled normally to 7 K (or 4 K) by means of a closed-cycle helium refrigerator. Typically, 1−5 mJ/pulse laser power was used. Nitric oxide (Matheson), $^{15}N^{16}O$ (MSD isotopes, 99%), and $^{14}N^{18}O$ (Isotec, 99%) were used to prepare the NO/Ar or NO/Ne mixtures. In general, matrix samples were deposited for 30−60 min with a typical rate of 2−4 mmol/h. After sample deposition, IR spectra were recorded on a BIO-RAD FTS-6000e spectrometer at 0.5 cm^{-1} resolution using a liquid-nitrogen-cooled HgCdTe (MCT) detector for the spectral range of 5000−400 cm^{-1}. Samples were annealed at different temperatures and subjected to broad-band irradiation ($\lambda > 250$ nm) using a high-pressure mercury arc lamp (Ushio, 100 W).

Quantum chemical calculations were performed to predict the structures and vibrational frequencies of the observed reaction products using the Gaussian 03 program.[14] The BP86 and B3LYP density functional methods were used.[15] 6-311+G(d) was used for N, O, Si, and Ge atoms,[16] and the Los Alamos ECP plus DZ (LANL2DZ) was used for Sn and Pb atoms.[17] Geometries were fully optimized, and vibrational frequencies were calculated with analytical second derivatives. The recent investigations have shown that such a computational strategy can provide reliable information for metal nitrosyl, such as infrared frequencies, relative absorption intensities, and isotopic shifts.[8]

Results and Discussion

Experiments have been done with NO concentrations ranging from 0.01% to 1.0% in excess argon and neon. Typical infrared spectra for the reactions of laser-ablated Sn and Pb atoms with NO molecules in excess argon and neon in the selected regions are illustrated in Figures 1−5, and the absorption bands in different isotopic experiments are

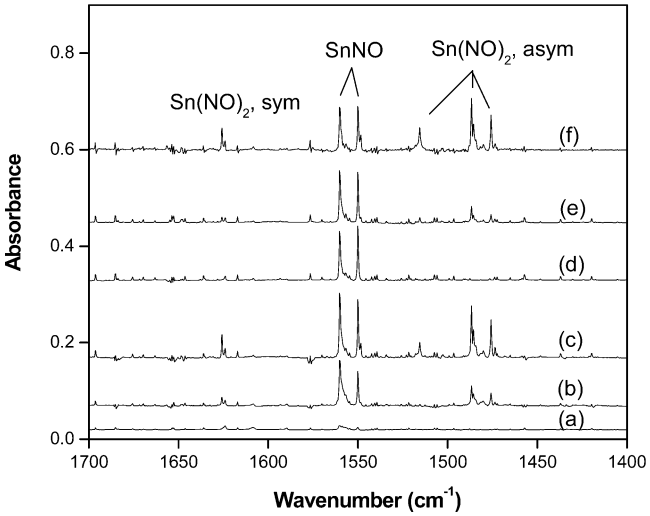

Figure 1. Infrared spectra in the 1700−1400 cm^{-1} region from the co-deposition of laser-ablated Sn atoms with 0.05% NO in Ar: (a) after 40 min sample deposition at 7 K, (b) after annealing to 25 K, (c) after annealing to 30 K, (d) after 12 min broad-band irradiation, (e) after annealing to 34 K, and (f) 0.05% NO + 0.01% CCl_4, after annealing to 30 K.

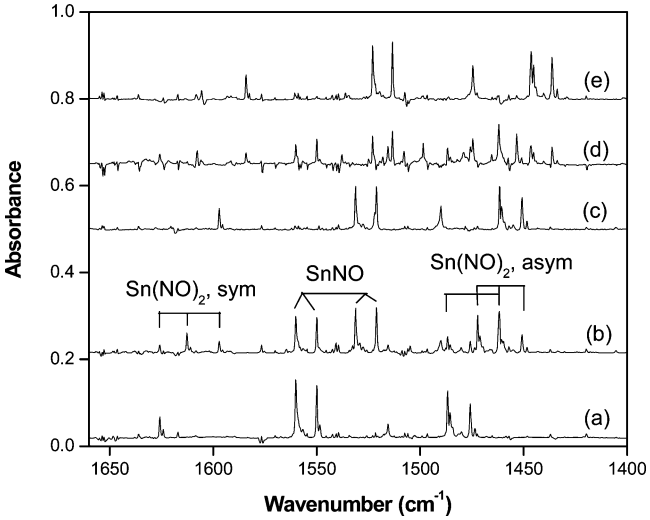

Figure 2. Infrared spectra in the 1650−1400 cm^{-1} region from the co-deposition of laser-ablated Sn atoms with isotopic NO in Ar after annealing to 30 K: (a) 0.05% $^{14}N^{16}O$, (b) 0.03% $^{14}N^{16}O$ + 0.03% $^{15}N^{16}O$, (c) 0.05% $^{15}N^{16}O$, (d) 0.03% $^{14}N^{16}O$ + 0.03% $^{14}N^{18}O$, and (e) 0.05% $^{14}N^{18}O$.

listed in Table 1. Metal independent absorptions due to the NO, $(NO)_2$, $(NO)_2^+$, $(NO)_2^-$, NO_2, NO^-, $(NO)_3^-$, and N_2O_3 species have been reported previously[18−20] and are not listed

(9) Zhou, M. F.; Tsumori, N.; Li, Z.; Fan, K.; Andrews, L.; Xu, Q. *J. Am. Chem. Soc.* **2002**, *124*, 12936. Zhou, M. F.; Xu, Q.; Wang, Z.; von Ragué Schleyer, P. *J. Am. Chem. Soc.* **2002**, *124*, 14854. Jiang, L.; Xu, Q. *J. Am. Chem. Soc.* **2005**, *127*, 42. Xu, Q.; Jiang, L.; Tsumori, N. *Angew. Chem., Int. Ed.* **2005**, *44*, 4338. Jiang, L.; Xu, Q. *J. Am. Chem. Soc.* **2005**, *127*, 8906.
(10) Zhou, M. F.; Jiang, L.; Xu, Q. *J. Phys. Chem. A* **2004**, *108*, 9521.
(11) Chou, J. B.; Bahou, M.; Lee, Y. P.; Rayner, D.; Simard, B. *J. Chem. Phys.* **2005**, *123*, 054321.
(12) Burkholder, T. R.; Andrews, L. *J. Chem. Phys.* **1991**, *95*, 8697.
(13) (a) Zhou, M. F.; Tsumori, N.; Andrews, L.; Xu, Q. *J. Phys. Chem. A* **2003**, *107*, 2458. (b) Jiang, L.; Xu, Q. *J. Chem. Phys.* **2005**, *122*, 034505.
(14) Frisch, M. J.; Trucks, G. W.; Schlegel, H. B.; Scuseria, G. E.; Robb, M. A.; Cheeseman, J. R.; Montgomery, J. A., Jr.; Vreven, T.; Kudin, K. N.; Burant, J. C.; Millam, J. M.; Iyengar, S. S.; Tomasi, J.; Barone, V.; Mennucci, B.; Cossi, M.; Scalmani, G.; Rega, N.; Petersson, G. A.; Nakatsuji, H.; Hada, M.; Ehara, M.; Toyota, K.; Fukuda, R.; Hasegawa, J.; Ishida, M.; Nakajima, T.; Honda, Y.; Kitao, O.; Nakai, H.; Klene, M.; Li, X.; Knox, J. E.; Hratchian, H. P.; Cross, J. B.; Adamo, C.; Jaramillo, J.; Gomperts, R.; Stratmann, R. E.; Yazyev, O.; Austin, A. J.; Cammi, R.; Pomelli, C.; Ochterski, J. W.; Ayala, P. Y.; Morokuma, K.; Voth, G. A.; Salvador, P.; Dannenberg, J. J.; Zakrzewski, V. G.; Dapprich, S.; Daniels, A. D.; Strain, M. C.; Farkas, O.; Malick, D. K.; Rabuck, A. D.; Raghavachari, K.; Foresman, J. B.; Ortiz, J. V.; Cui, Q.; Baboul, A. G.; Clifford, S.; Cioslowski, J.; Stefanov, B. B.; Liu, G.; Liashenko, A.; Piskorz, P.; Komaromi, I.; Martin, R. L.; Fox, D. J.; Keith, T.; Al-Laham, M. A.; Peng, C. Y.; Nanayakkara, A.; Challacombe, M.; Gill, P. M. W.; Johnson, B.; Chen, W.; Wong, M. W.; Gonzalez, C.; Pople, J. A. *Gaussian 03*, revision B.04; Gaussian, Inc.: Pittsburgh, PA, 2003.

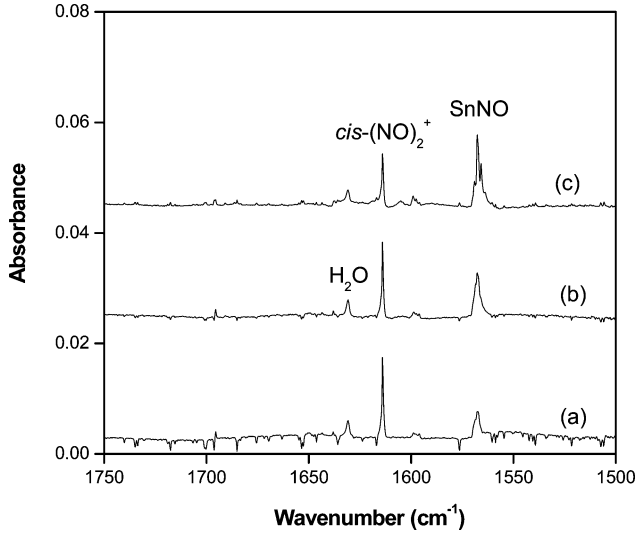

Figure 3. Infrared spectra in the 1750−1500 cm^{-1} region from the co-deposition of laser-ablated Sn atoms with 0.025% NO in Ne: (a) after 30 min sample deposition at 4 K, (b) after annealing to 6 K, and (e) after annealing to 8 K.

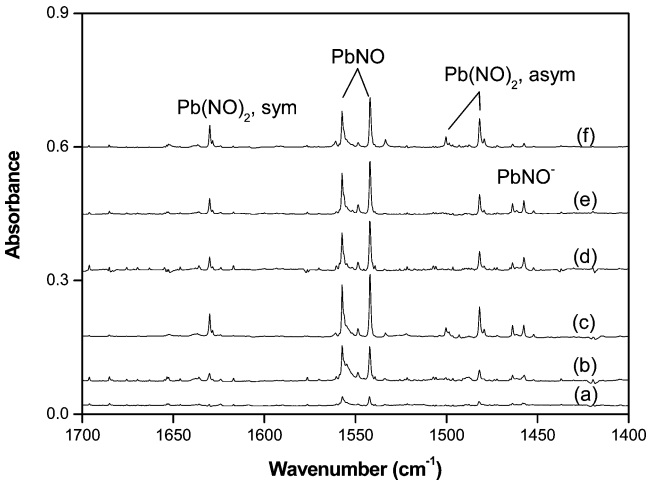

Figure 4. Infrared spectra in the 1700−1400 cm^{-1} region from the co-deposition of laser-ablated Pb atoms with 0.05% NO in Ar: (a) after 40 min sample deposition at 7 K, (b) after annealing to 25 K, (c) after annealing to 30 K, (d) after 12 min broad-band irradiation, (e) after annealing to 34 K, and (f) 0.05% NO + 0.01% CCl_4, after annealing to 30 K.

here. The stepwise annealing and photolysis behavior of the product absorptions is also shown in the figures and will be discussed below. Experiments were also done with different concentrations of CCl_4 serving as an electron scavenger.

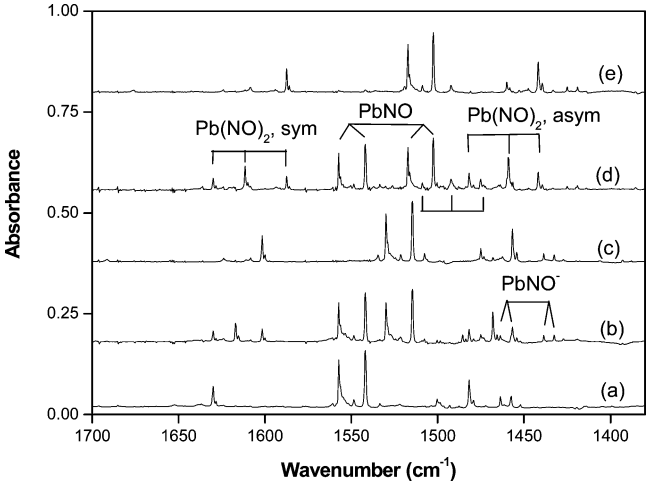

Figure 5. Infrared spectra in the 1700−1400 cm^{-1} region from the co-deposition of laser-ablated Pb atoms with isotopic NO in Ar after annealing to 30 K: (a) 0.05% $^{14}N^{16}O$, (b) 0.03% $^{14}N^{16}O$ + 0.03% $^{15}N^{16}O$, (c) 0.05% $^{15}N^{16}O$, (d) 0.03% $^{14}N^{16}O$ + 0.03% $^{14}N^{18}O$, and (e) 0.05% $^{14}N^{18}O$.

Quantum chemical calculations have been carried out for the possible isomers and electronic states of the potential product molecules. Figure 6 shows the optimized structures, electronic ground state, point group, and the relative energies of the $M(NO)_n$ and MNO^- (M = Sn, Pb; n = 1, 2) isomers. Table 2 reports a comparison of the observed and calculated isotopic frequency ratios for the N−O stretching modes of the reaction products. The representative ground electronic states, point groups, vibrational frequencies, and intensities calculated at the BP86/6-311+G(d)-LANL2DZ level are listed in Table 3. Molecular orbital depictions of the highest occupied molecular orbitals (HOMO) of the $M(NO)_n$ (M = Sn, Pb; n = 1, 2) and $PbNO^-$ molecules are illustrated in Figure 7.

SnNO. The absorptions at 1560.1 and 1550.0 cm^{-1} weakly appear during sample deposition, markedly increase upon annealing, slightly decrease after broad-band irradiation, and slightly increase after further annealing to 34 K (Table 1 and Figure 1). These two bands respectively shift to 1531.2 and 1521.1 cm^{-1} with $^{15}N^{16}O$ and to 1523.0 and 1521.1 cm^{-1} with $^{14}N^{18}O$, exhibiting isotopic frequency ratios ($^{14}N^{16}O/^{15}N^{16}O$, 1.0189 and 1.0190; $^{14}N^{16}O/^{14}N^{18}O$, 1.0244 and 1.0242) characteristic of N−O stretching vibrations.[8] As shown in Figure 2, the mixed $^{14}N^{16}O$ + $^{15}N^{16}O$ and $^{14}N^{16}O$ + $^{14}N^{18}O$ isotopic spectra only provide the sum of pure isotopic bands, which indicates a mononitrosyl molecule.[21] On the basis of the growth/decay characteristics as a function of changes of experimental conditions, the absorptions at 1560.1 and 1550.0 cm^{-1} can be grouped together to one species. Doping with CCl_4 has no effect on these bands (Figure 1, trace f), suggesting that the product is neutral.[8] The 1560.1 and 1550.0 cm^{-1} bands are therefore assigned to the N−O stretching vibration of the neutral tin mononitrosyl SnNO in different matrix sites.[8] The corresponding N−O stretching frequency of SnNO in solid neon has been observed at 1567.7 cm^{-1} (Figure 3), which is 7.6 cm^{-1} blue-shifted from the present argon matrix counterpart (1560.1 cm^{-1}).

(15) Becke, A. D. *Phys. Rev. A: At., Mol., Opt. Phys.* **1988**, *38*, 3098. Perdew, J. P. *Phys. Rev. B: Condens. Matter Mater. Phys.* **1986**, *33*, 8822. Lee, C.; Yang, E.; Parr, R. G. *Phys. Rev. B: Condens. Matter Mater. Phys.* **1988**, *37*, 785. Becke, A. D. *J. Chem. Phys.* **1993**, *98*, 5648.
(16) McLean, A. D.; Chandler, G. S. *J. Chem. Phys.* **1980**, *72*, 5639. Krishnan, R.; Binkley, J. S.; Seeger, R.; Pople, J. A. *J. Chem. Phys.* **1980**, *72*, 650.
(17) Wachter, J. H. *J. Chem. Phys.* **1970**, *52*, 1033. Hay, P. J. *J. Chem. Phys.* **1977**, *66*, 4377. Hay, P. J.; Wadt, W. R. *J. Chem. Phys.* **1985**, *82*, 299.
(18) Andrews, L.; Zhou, M. F.; Willson, S. P.; Kushto, G. P.; Snis, A.; Panas, I. *J. Chem. Phys.* **1998**, *109*, 177 (argon) and references therein.
(19) Lugez, C. L.; Thompson, W. E.; Jacox, M. E.; Snis, A.; Panis, I. *J. Chem. Phys.* **1999**, *110*, 10345 (neon) and references therein.
(20) Andrews, L.; Zhou, M. F. *J. Chem. Phys.* **1999**, *111*, 6036 (neon) and references therein.
(21) Darling, J. H.; Ogden, J. S. *J. Chem. Soc., Dalton Trans.* **1972**, 2496.

Table 1. Infrared Absorptions (cm^{-1}) Observed after the Co-Deposition of Laser-Ablated Tin and Lead Atoms with NO in Excess Argon at 7 K

$^{14}N^{16}O$	$^{15}N^{16}O$	$^{14}N^{18}O$	$^{14}N^{16}O + {}^{15}N^{16}O$	$^{14}N^{16}O + {}^{14}N^{18}O$	*R* (14/15)	*R* (16/18)	assignment
1625.8	1597.1	1584.1	1625.8, 1612.7, 1597.1	1625.8, 1607.7, 1584.1	1.0180	1.0263	$Sn(NO)_2$, *s*-NO str.[a]
1560.1	1531.2	1523.0	1560.1, 1531.2	1560.1, 1523.0	1.0189	1.0244	SnNO, NO str.
1550.0	1521.1	1513.4	1550.0, 1521.1	1550.0, 1513.4	1.0190	1.0242	SnNO site, NO str.
1515.5	1490.0	1474.5	1515.5, 1504.9, 1490.0	1515.5, 1498.5, 1474.5	1.0171	1.0278	$Sn(NO)_2$ site, *as*-NO str.
1486.7	1461.7	1446.3	1486.7, 1472.2, 1461.9	1486.7, 1462.1, 1446.3	1.0171	1.0279	$Sn(NO)_2$, *as*-NO str.
1475.8	1450.8	1436.2	1475.9, 1461.9, 1450.8	1475.8, 1453.3, 1436.2	1.0172	1.0276	$Sn(NO)_2$ site, *as*-NO str.
1630.0	1601.6	1587.5	1630.0, 1617.0, 1601.6	1630.0, 1611.5, 1587.5	1.0177	1.0268	$Pb(NO)_2$, *s*-NO str.
1557.3	1529.9	1517.3	1557.3, 1529.9	1557.3, 1517.3	1.0179	1.0264	PbNO site, NO str.
1541.9	1514.7	1502.6	1541.9, 1514.7	1541.9, 1502.6	1.0180	1.0262	PbNO, NO str.
1500.4	1475.0	1460.0	1500.4, 1485.6, 1475.0	1500.4, 1492.3, 1460.0	1.0172	1.0278	$Pb(NO)_2$ site, *as*-NO str.
1481.8	1456.8	1441.9	1481.8, 1468.1, 1456.8	1481.8, 1459.0, 1441.9	1.0172	1.0277	$Pb(NO)_2$, *as*-NO str.
1463.7	1438.6	1425.0	1463.7, 1438.6	1463.7, 1425.0	1.0174	1.0272	$PbNO^-$ site, NO str.
1457.5	1432.5	1419.1	1457.5, 1432.5	1457.5, 1419.1	1.0175	1.0271	$PbNO^-$, NO str.

[a] Abbreviations: as = asymmetric, s = symmetric, and str. = stretching mode.

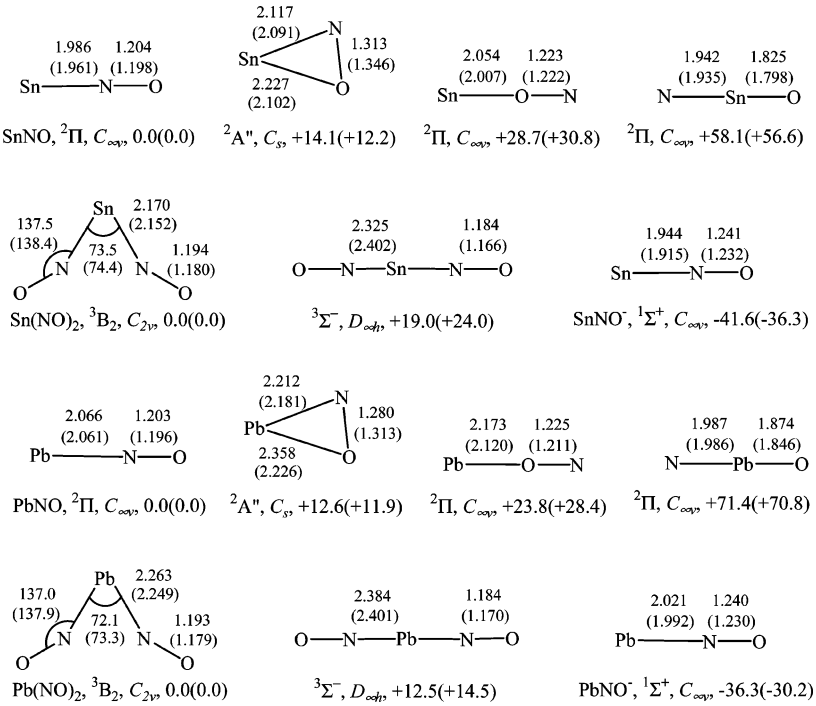

Figure 6. Optimized structures (bond length in angstroms and bond angle in degrees), electronic ground state, point group, and the relative energies (in kilocalories per mole) of the $M(NO)_n$ and MNO^- (M = Sn, Pb; n = 1, 2) isomers calculated at the BP86/6-311+G(d)-LANL2DZ and B3LYP/6-311+G(d)-LANL2DZ (in parentheses) levels.

Table 2. Comparison of Observed and Calculated N−O Stretching Modes of the Tin and Lead Nitrosyls

		experimental			calculated			
species	ν_{N-O} mode	freq (cm^{-1})	*R* (14/15)	*R* (16/18)	method	freq (cm^{-1})	*R* (14/15)	*R* (16/18)
SnNO	σ	1560.1	1.0189	1.0244	BP86	1589.1	1.0192	1.0253
					B3LYP	1608.0	1.0189	1.0256
$Sn(NO)_2$	a_1	1625.8	1.0180	1.0263	BP86	1658.3	1.0185	1.0264
					B3LYP	1739.5	1.0185	1.0265
$Sn(NO)_2$	b_2	1486.7	1.0171	1.0279	BP86	1587.0	1.0176	1.0280
					B3LYP	1648.9	1.0174	1.0284
PbNO	σ	1541.9	1.0180	1.0262	BP86	1586.0	1.0188	1.0259
					B3LYP	1615.0	1.0186	1.0263
$Pb(NO)_2$	a_1	1630.0	1.0177	1.0268	BP86	1654.0	1.0183	1.0266
					B3LYP	1734.2	1.0183	1.0268
$Pb(NO)_2$	b_2	1481.8	1.0172	1.0277	BP86	1590.1	1.0177	1.0280
					B3LYP	1657.5	1.0175	1.0282
$PbNO^-$	σ	1457.5	1.0175	1.0271	BP86	1436.2	1.0195	1.0248
					B3LYP	1460.1	1.0193	1.0248

Density functional theory (DFT) calculations of four different geometric SnNO isomers with different electronic states (i.e., end-bonded SnNO, side-bonded *cyc*-SnNO, isonitrosyl SnON, and inserted NSnO) have been preformed at the BP86/6-311+G(d)-LANL2DZ and B3LYP/6-311+G(d)-LANL2DZ levels (Figure 6). When BP86 calculated results are taken as an example, all four of the SnNO isomers are predicted to be stable relative to the ground-state Sn atom and NO molecule, and all have a doublet ground state. The end-bonded SnNO nitrosyl is the global minimum, whereas

Table 3. Ground Electronic States, Point Groups, Vibrational Frequencies (cm^{-1}), and Intensities (km/mol) of the Reaction Products Calculated at the BP86/6-311+G(d)-LANL2DZ Level

species	elec state	point group	frequencies (intensity, mode)
SnNO	$^2\Pi$	$C_{\infty v}$	1589.1 (610, σ), 408.4 (7, σ), 261.7 (24, π), 212.0 (5, π)
$Sn(NO)_2$	$^3B_2$	C_{2v}	1658.3 (376, A_1), 1587.0 (1185, B_2), 393.9 (0, A_2), 382.7 (5, A_1), 314.8 (0.1, B_2), 274.4 (0.1, A_1), 228.4 (0.01, B_2), 131.1 (2, B_1), 96.4 (0.4, A_1)
PbNO	$^2\Pi$	$C_{\infty v}$	1586.0 (714, σ), 353.1 (5, σ), 245.4 (29, π), 204.0 (8, π)
$Pb(NO)_2$	$^3B_2$	C_{2v}	1654.0 (466, A_1), 1590.1 (1339, B_2), 373.6 (0, A_2), 352.7 (1, A_1), 297.4 (10, B_2), 242.3 (0.5, A_1), 200.5 (0.01, B_2), 119.9 (4, B_1), 82.4 (0.3, A_1)
$PbNO^-$	$^1\Sigma^+$	$C_{\infty v}$	1436.2 (915, σ), 376.7 (16, σ), 281.3 (45× 2, π)

the *cyc*-SnNO, SnON, and NSnO isomers are 14.1, 28.7, and 58.1 kcal/mol higher in energy, respectively. Furthermore, the doublet SnNO lies 25.9 kcal/mol lower in energy than the quartet one. The calculated ν_{N-O} value (1589.1 cm^{-1}, Tables 2 and 3) of the doublet SnNO shows a scale factor (the ratio of the observed frequency to the calculated frequency) of 0.982, which is typical for this functional and class of molecules.[8] As shown in Table 3, the Sn−N stretching frequency of the doublet SnNO is calculated at 408.4 cm^{-1}, while its intensity (7 km/mol) is too small to be detected. Equally as important, the calculated $^{14}N^{16}O/^{15}N^{16}O$ and $^{14}N^{16}O/^{14}N^{18}O$ isotopic frequency ratios of 1.0192 and 1.0253 are in accord with the experimental observations, 1.0189 and 1.0244, respectively. These good agreements substantiate the identification of this doublet tin mononitrosyl SnNO from the matrix IR spectra. Good agreements between the experimental and calculated results have also been obtained at the B3LYP/6-311+G(d)-LANL2DZ level (Table 2 and Figure 6). Recent studies indicate that, in most cases, the BP86 functional gives calculated ν_{C-O} and ν_{N-O} frequencies much closer to the experimental values than the B3LYP functional.[8,22] Hereafter, mainly BP86 results are presented for discussions.

$Sn(NO)_2$. The absorptions at 1625.8 and 1486.7 cm^{-1} (Table 1 and Figure 1) with two matrix trapping sites at 1515.5 and 1475.8 cm^{-1} are present together after sample annealing, disappear after broad-band irradiation, and slightly recover after further annealing to 34 K. These two main bands respectively shift to 1597.1 and 1461.7 cm^{-1} with $^{15}N^{16}O$ and to 1584.1 and 1446.3 cm^{-1} with $^{14}N^{18}O$, exhibiting isotopic frequency ratios ($^{14}N^{16}O/^{15}N^{16}O$, 1.0180 and 1.0171; $^{14}N^{16}O/^{14}N^{18}O$, 1.0263 and 1.0279) characteristic of N−O stretching vibrations.[8] As can be seen in Figure 2, two sets of triplet bands have been observed at 1625.8/1612.7/1597.1 and 1486.7/1472.2/1461.9 cm^{-1} in the mixed $^{14}N^{16}O + ^{15}N^{16}O$ isotopic spectra (Table 1). Similar isotopic spectra in the $^{14}N^{16}O + ^{14}N^{18}O$ experiments have also been observed. Doping with CCl_4 has no effect on these bands (Figure 1, trace f), suggesting that the product is neutral.[8] Accordingly, these bands are assigned to the symmetric and antisymmetric N−O stretching modes of the $Sn(NO)_2$ molecule. It is noted that the antisymmetric N−O stretching bands have relatively large intensities, and therefore, their matrix trapping sites are readily observable, whereas the symmetric N−O stretching bands have much smaller intensities so that their matrix trapping sites are difficult to resolve. The absorptions of the $Sn(NO)_2$ molecule are absent from the present neon experiments.

Our BP86 calculations predict that the $Sn(NO)_2$ molecule has a $^3B_2$ ground state with C_{2v} symmetry, which lies 19.0 kcal/mol lower in energy than the linear one (Figure 6). The ∠NMN bond angle is 73.5°, which is slightly smaller than that in $Si(NO)_2$ (83.7°)[10] and $Ge(NO)_2$ (76.8°).[11] The symmetric and antisymmetric N−O stretching vibrational frequencies are calculated at 1658.3 and 1587.0 cm^{-1} (Tables 2 and 3), which must be scaled down by 0.980 and 0.937 to fit the experimental frequencies, 1625.8 and 1486.7 cm^{-1}, respectively. For the antisymmetric N−O stretching mode, however, the calculated $^{14}N^{16}O/^{15}N^{16}O$ and $^{14}N^{16}O/^{14}N^{18}O$ isotopic frequency ratios of 1.0185 and 1.0264 (Table 2) are consistent with the experimental observations, 1.0180 and 1.0263, respectively. Similar results have also been obtained for the symmetric N−O stretching mode. These agreements between the experimental and calculated vibrational frequencies, relative absorption intensities, and isotopic shifts confirm the identification of the $Sn(NO)_2$ molecule from the matrix IR spectra.

PbNO. Two weak bands at 1557.3 and 1541.9 cm^{-1} appear together during sample deposition, sharply increase upon annealing, slightly decrease after broad-band irradiation, and slightly increase after further annealing to 34 K (Table 1 and Figure 4). These two bands respectively shift to 1529.9 and 1514.7 cm^{-1} with $^{15}N^{16}O$ and to 1517.3 and 1502.6 cm^{-1} with $^{14}N^{18}O$. The isotopic frequency ratios ($^{14}N^{16}O/^{15}N^{16}O$, 1.0179 and 1.0180; $^{14}N^{16}O/^{14}N^{18}O$, 1.0264 and 1.0262) imply that these two bands are mainly due to an N−O stretching mode.[8] Only the pure isotopic counterparts have been presented in the mixed $^{14}N^{16}O + ^{15}N^{16}O$ and $^{14}N^{16}O + ^{14}N^{18}O$ isotopic spectra (Figure 5), suggesting that only one NO subunit is involved in this mode.[21] Doping with CCl_4 has no effect on these bands (Figure 4, trace f), indicating that the product is neutral.[8] On the basis of the growth/decay

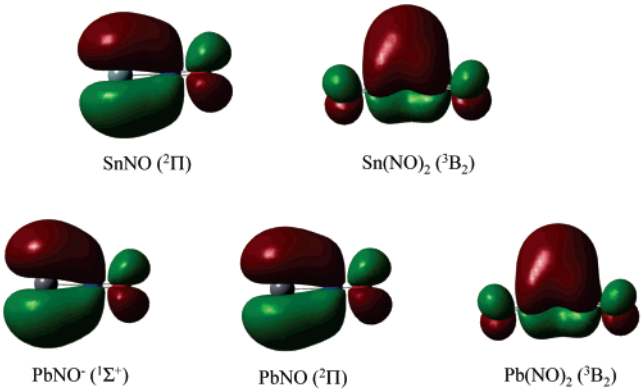

Figure 7. Molecular orbital depictions of the HOMOs of the $M(NO)_n$ (M = Sn, Pb; n = 1, 2) and $PbNO^-$ molecules.

(22) Bauschlicher, C. W., Jr.; Ricca, A.; Partridge, H.; Langhoff, S. R. In *Recent Advances in Density Functional Theory, Part II*; Chong, D. P., Ed.; World Scientific Publishing: Singapore, 1997. Bytheway, I.; Wong, M. W. *Chem. Phys. Lett.* **1998**, *282*, 219.

characteristics as a function of changes of experimental conditions, the absorptions at 1557.3 and 1541.9 cm^{-1} can be grouped together to one species. The 1557.3 and 1541.9 cm^{-1} bands are therefore assigned to the N−O stretching vibration of the neutral PbNO molecule in different matrix sites. The corresponding N−O stretching frequency of PbNO in solid neon has been observed at 1564.7 cm^{-1} (not shown here), which is 22.8 cm^{-1} blue-shifted from the present argon matrix counterpart (1541.9 cm^{-1}).

The present DFT calculations lend strong support for the assignment of PbNO. The PbNO molecule is predicted to have a doublet ground state with a linear structure, similar to MNO (M = Si,[10] Ge,[11] and Sn). The doublet PbNO lies 21.3 kcal/mol lower in energy than the quartet one. The *cyc*-PbNO, PbON, and NPbO isomers are respectively 12.6, 23.8, and 71.4 kcal/mol higher in energy than the end-bonded one. The calculated N−O stretching frequency (1586.0 cm^{-1}, Tables 2 and 3) is consistent with the experimental values (1557.3 and 1541.9 cm^{-1}). The Pb−N stretching frequency of the doublet PbNO is predicted to be 353.1 cm^{-1}, which is beyond the present spectral range of 5000−400 cm^{-1}. The calculated $^{14}N^{16}O/^{15}N^{16}O$ and $^{14}N^{16}O/^{14}N^{18}O$ isotopic frequency ratios of 1.0188 and 1.0259 are in accord with the experimental observations, 1.0180 and 1.0262, respectively.

Pb(NO)$_2$. The absorptions at 1630.0 and 1481.8 cm^{-1} (Table 1 and Figure 4) with a matrix trapping site at 1500.4 cm^{-1} are present together after sample annealing, disappear after broad-band irradiation, and slightly recover after further annealing to 34 K. These two main bands respectively shift to 1601.6 and 1456.8 cm^{-1} with $^{15}N^{16}O$ and to 1587.5 and 1441.9 cm^{-1} with $^{14}N^{18}O$, exhibiting isotopic frequency ratios ($^{14}N^{16}O/^{15}N^{16}O$, 1.0177 and 1.0172; $^{14}N^{16}O/^{14}N^{18}O$, 1.0268 and 1.0277) characteristic of N−O stretching vibrations. The mixed isotopic spectra give two sets of triplet bands with 1:2:1 relative intensities (Table 1, Figure 5), which denote two equivalent NO subgroups.[21] Doping with CCl_4 has no effect on these bands (Figure 4, trace f), suggesting that the product is neutral.[8] Accordingly, these bands are assigned to the symmetric and antisymmetric N−O stretching modes of the Pb(NO)$_2$ molecule. However, the neon matrix counterpart is absent from the present experiments.

Analogous to M(NO)$_2$ (M = Si,[10] Ge,[11] Sn), the Pb(NO)$_2$ molecule has a $^3B_2$ ground state with C_{2v} symmetry, which lies 12.5 kcal/mol lower in energy than the linear one (Figure 6). The ∠NMN bond angle is predicted to be 72.1°. It is interesting to note that the ∠NMN bond angles in the M(NO)$_2$ molecules show a monotonic decrease (i.e., Si, 83.7°;[10] Ge, 76.8°;[11] Sn, 73.5°; and Pb, 72.1°) going down the Si family. The symmetric and antisymmetric N−O stretching vibrational frequencies of Pb(NO)$_2$ are calculated at 1654.0 and 1590.1 cm^{-1} (Tables 2 and 3), which are in accord with our observed values, 1630.0 and 1481.8 cm^{-1}, respectively. As listed in Table 2, the calculated $^{14}N^{16}O/^{15}N^{16}O$ and $^{14}N^{16}O/^{14}N^{18}O$ isotopic frequency ratios are also consistent with the experimental observations. The assignment of the Pb(NO)$_2$ molecule is supported by these agreements between the experimental and calculated vibrational frequencies, relative absorption intensities, and isotopic shifts.

PbNO$^-$. The absorptions at 1463.7 and 1457.5 cm^{-1} appear during sample annealing (Table 1 and Figure 4). These bands respectively shift to 1438.6 and 1432.5 cm^{-1} with $^{15}N^{16}O$ and to 1425.0 and 1419.1 cm^{-1} with $^{14}N^{18}O$. The isotopic frequency ratios ($^{14}N^{16}O/^{15}N^{16}O$, 1.0174 and 1.0175; $^{14}N^{16}O/^{14}N^{18}O$, 1.0272 and 1.0271) imply that these two bands are mainly due to an N−O stretching mode.[8] Only the pure isotopic counterparts have been observed in the mixed $^{14}N^{16}O + ^{15}N^{16}O$ and $^{14}N^{16}O + ^{14}N^{18}O$ isotopic spectra (Figure 5), suggesting that only one NO subunit is involved in this mode.[21] On the basis of the growth/decay characteristics as a function of changes of experimental conditions, the absorptions at 1463.7 and 1457.5 cm^{-1} can be grouped together to one species. Doping with CCl_4 decreases these bands (Figure 4, trace f), suggesting that the product is anionic.[8] The 1463.7 and 1457.5 cm^{-1} bands are therefore assigned to the N−O stretching vibration of the PbNO$^-$ anion in different matrix sites. It is noted that, at the present experimental conditions, the PbNO$^-$ anion is observed but its silicon,[10] germanium,[11] and tin counterparts are not observed. Further investigation is helpful to elucidate this aspect.

Our DFT calculations predict the PbNO$^-$ anion to have a $^1\Sigma_g^+$ ground state with $C_{\infty v}$ symmetry (Table 2 and Figure 6). The N−O stretching mode of the PbNO$^-$ species is calculated at 1436.2 cm^{-1} (Table 2), which is lower than the observed values (1463.7 and 1457.5 cm^{-1}). The calculated $^{14}N^{16}O/^{15}N^{16}O$ and $^{14}N^{16}O/^{14}N^{18}O$ isotopic frequency ratios are consistent with the experimental observations. The Pb−N stretching frequency of the PbNO$^-$ anion is predicted to be 376.7 cm^{-1}, which is beyond the present spectral range of 5000−400 cm^{-1}.

Reaction Mechanism

At the present experimental conditions, laser-ablated tin and lead atoms react with nitric oxide molecules in the excess argon and neon matrices to produce metal nitrosyl species. For the Sn + NO reaction in solid argon, the Sn(NO)$_n$ (n = 1, 2) molecules are the primary products after sample annealing, suggesting that reactions 1 and 2 require little or no activation energy. Interestingly, the absorptions of Sn(NO)$_2$ increase upon sample annealing at the expense of *cis*-(NO)$_2$ (1866.3 and 1777.9 cm^{-1},[20] not shown here), indicating that the Sn(NO)$_2$ molecule is most probably formed via the combination of a Sn atom with the *cis*-(NO)$_2$ (reaction 3). Furthermore, reaction 3 (−50 kcal/mol) is predicted to be more energetically favorable than reaction 2 (−19 kcal/mol), which supports the above-mentioned analysis.

$$\mathrm{Sn}\ (^3P_0) + \mathrm{NO}\ (^2\Pi) \rightarrow \mathrm{SnNO}\ (^2\Pi)\ (\Delta E = -46\ \text{kcal/mol, BP86 level}) \quad (1)$$

$$\mathrm{SnNO}\ (^2\Pi) + \mathrm{NO}\ (^2\Pi) \rightarrow \mathrm{Sn(NO)_2}\ (^3B_2)\ (\Delta E = -19\ \text{kcal/mol}) \quad (2)$$

$$\mathrm{Sn}\ (^3P_0) + \textit{cis}\text{-}(\mathrm{NO})_2\ (^3B_1) \rightarrow \mathrm{Sn(NO)_2}\ (^3B_2)\ (\Delta E = -50\ \text{kcal/mol}) \quad (3)$$

Besides the neutral Pb(NO)$_n$ (n = 1, 2) species, the matrix argon experiment of the lead system yields the PbNO$^-$ anion.

Similar to the Sn system, the reactions of lead atoms with NO molecules are predicted to be exothermic (reactions 4−7), implying that the formation of lead nitrosyls is energetically favorable.

$$Pb\ (^3P_0) + NO\ (^2\Pi) \rightarrow PbNO\ (^2\Pi)\ (\Delta E = -41\ \text{kcal/mol}) \quad (4)$$

$$PbNO\ (^2\Pi) + e^- \rightarrow PbNO^-\ (^1\Sigma^+)\ (\Delta E = -36\ \text{kcal/mol}) \quad (5)$$

$$PbNO\ (^2\Pi) + NO\ (^2\Pi) \rightarrow Pb(NO)_2\ (^3B_2)\ (\Delta E = -18\ \text{kcal/mol}) \quad (6)$$

$$Pb\ (^3P_0) + \textit{cis}\text{-}(NO)_2\ (^3B_1) \rightarrow Pb(NO)_2\ (^3B_2)\ (\Delta E = -44\ \text{kcal/mol}) \quad (7)$$

We also note that only the end-bonded nitrosyls have been observed for Ge,[11] Sn, and Pb, whereas three different SiNO isomers,[10] namely, the end-bonded SiNO, the side-bonded *cyc*-SiNO, and the inserted NSiO, have been observed for Si. This suggests that the isomerization of heavier MNO (M = Ge, Sn, Pb) is more difficult than that of SiNO.

As illustrated in Figure 7, the HOMOs in the $M(NO)_n$ (M = Sn, Pb; n = 1, 2) and $PbNO^-$ molecules are the M−N π-bonding orbitals, which are responsible for the stability of these metal nitrosyls. We also note that the yields of lead nitrosyls are larger than those of lead carbonyls,[13b] implying that NO is more reactive with Pb than CO. This may be explained by stating that one unpaired electron in a π^* orbital in the NO molecule makes it more reactive than other diatomic molecules such as CO. It is interesting to note that the N−O stretching vibrational frequencies of MNO (M = Si, Ge, Sn, and Pb) decrease from SiNO to PbNO with the exception of SnNO (1548.7,[10] 1543.8,[11] 1560.1, and 1541.9 cm^{-1}), which indicates an increasing in metal-to-nitrosyl back-bonding in this series. In contrast, the increase in MCO carbonyl frequencies has been observed from Si to Pb (1898.1, 1907.4, 1941.1, and 2027.7 cm^{-1}).[13b,23]

It is also noteworthy that only 1:1 metal/NO adducts are observed in the Ne matrix, while both 1:1 and 1:2 metal/NO adducts are observed in the Ar matrix. Recent investigations exhibit that some metal nitrosyls (Nb, Ta, Mo, W, Re, etc.) are more readily stabilized in solid argon than in solid neon.[8] Insights into this trend may be obtained from systematic investigations on metal nitrosyls in different noble gas matrices.

Conclusions

Laser-ablated tin and lead atoms react with nitric oxide molecules in the excess argon and neon matrices to produce metal nitrosyl species. On the basis of the isotopic shifts and splitting patterns, the $M(NO)_n$ (M = Sn, Pb; n = 1, 2) and $PbNO^-$ molecules have been characterized in the present argon experiments. Matrix neon experiments only give the SnNO and PbNO products. Density functional theory calculations have been performed on the tin and lead nitrosyls, which lend strong support to the experimental assignments of the infrared spectra. Furthermore, the plausible reaction mechanism for the formation of these metal nitrosyls has been proposed. Bonding analysis shows that the HOMOs in the $M(NO)_n$ (M = Sn, Pb; n = 1, 2) and $PbNO^-$ molecules are the M−N π-bonding orbitals.

Acknowledgment. We thank Prof. Mingfei Zhou for helpful discussions. This work was supported by a Grant-in-Aid for Scientific Research (B) (Grant No. 17350012) from the Ministry of Education, Culture, Sports, Science and Technology (MEXT) of Japan. L.J. thanks the MEXT of Japan and Kobe University for an Honors Scholarship.

IC061105R

(23) Zhang, L. N.; Dong, J.; Zhou, M. F. *J. Chem. Phys.* **2000**, *113*, 8700.